Using Spherical Harmonics for Modeling Antenna Patterns

Arne Schmitz
Computer Graphics Group
RWTH Aachen University
Email: aschmitz@cs.rwth-aachen.de

Thomas Karolski
Computer Graphics Group
RWTH Aachen University
Email: thomas.karolski@rwth-aachen.de

Leif Kobbelt
Computer Graphics Group
RWTH Aachen University
Email: kobbelt@cs.rwth-aachen.de

***Abstract*—In radio wave propagation simulations there is a need for modeling antenna patterns. Both the transmitting and the receiving antenna influence the wireless link. We use spherical harmonics to compress the amount of measured data needed for complex antenna patterns. We present a method to efficiently incorporate these patterns into a ray tracing framework for radio wave propagation. We show how to efficiently generate rays according to the transmitting antenna pattern. The ray tracing simulation computes a compressed irradiance field for every point in the scene. The receiving antenna pattern can then be applied to this field for the final estimation of signal strength.**

***Index Terms*—Antenna radiation patterns; Radio propagation; Ray tracing**

I. Introduction

For propagation simulations to be accurate, the radiation patterns of both the transmitting as well as the receiving antenna are very important. Most antennas have directional characteristics, however many simulations still assume isotropic antennas. There are several problems to overcome when one wants to implement full support for directional antennas in a ray tracing framework. First of all, antenna pattern measurements often consist of thousands of data samples. Sampling those antenna patterns for ray shooting at a transmitting antenna (Tx) is costly. Second, computing the product of an irradiance field with a receiving antenna (Rx) pattern can become computationally very expensive as well.

We propose to use spherical harmonics (SH) for both the Tx and Rx antenna pattern as well as for the irradiance field computed by the ray tracing simulation. The SH basis allows for fast sample warping of the rays launched at the Tx antenna. It also allows us to compute the product of the irradiance field and the Rx antenna, giving us an entirely direction dependent representation of the received signal strength.

II. Related Work

Modeling antenna patterns has already been researched. Most similar to our approach are the works of Landmann et al. [1] and Rahola et al. [2]. While achieving good results in reconstructing patterns, Landmann's approach has the disadvantage of not choosing a basis on the sphere. Depending on the rotation of the antenna, the approximation quality of their Effective Aperture Distribution Function (EADF) varies. This is not the case in the SH basis. Rotations are easily achieved, without loss of accuracy. Rahola only describes how to express antenna patterns in the SH basis, but does not continue to explain how to incorporate this into a radio propagation framework.

Another method of synthesizing antenna patterns is given by Chang [3]. Here, the spherical Bessel functions are used as basis functions.

An application of a system supporting arbitrary antenna patterns is given by Sheth et al. [4]. The authors present a method of limiting the covered area of WiFi base stations by using directional antennas and the simulation of those.

Similarly, Boerman et al. [5] explored reconfigurable antenna patterns in MIMO communication systems. Being able to model different antenna patterns is vital in this kind of research. Another example of this is presented by Gunnarsson et al. [6], where simple augmentation of HSPA and LTE antenna patterns are used to predict the performance of real networks.

In this work we will concentrate on the antenna pattern models and their integration into ray tracing frameworks. The impact of this on network simulations remains to be researched.

III. Spherical Harmonics

Spherical harmonics form an orthonormal basis of the square-integrable functions $L^2(S)$ on a sphere. As such they have been used widely as an efficient method for approximately and compactly representing spherical functions. A good practical guide for using SH in the context of ray tracing (for rendering) has been presented by Green [7]. The basis function for degree $l \geq 0$ and order m (with $-l \leq m \leq l$) is defined as:

$$y_l^m(\theta,\phi) = \begin{cases} \sqrt{2}K_l^m \cos(m\phi)P_l^m(\cos\theta) & m > 0 \\ K_l^0 P_l^0(\cos\theta) & m = 0 \\ \sqrt{2}K_l^m \sin(-m\phi)P_l^{-m}(\cos\theta) & m < 0 \end{cases} \quad (1)$$

Where K_l^m is a normalization term and P_l^m are the associated Legendre polynomials. The different degrees l represent functions of different frequencies on the sphere. The process of computing the representation of a spherical function $f(s)$ in the SH basis is called projection, and gives us the SH coefficients c_l^m:

$$c_l^m = \int_S f(s) y_l^m(s) ds \quad (2)$$

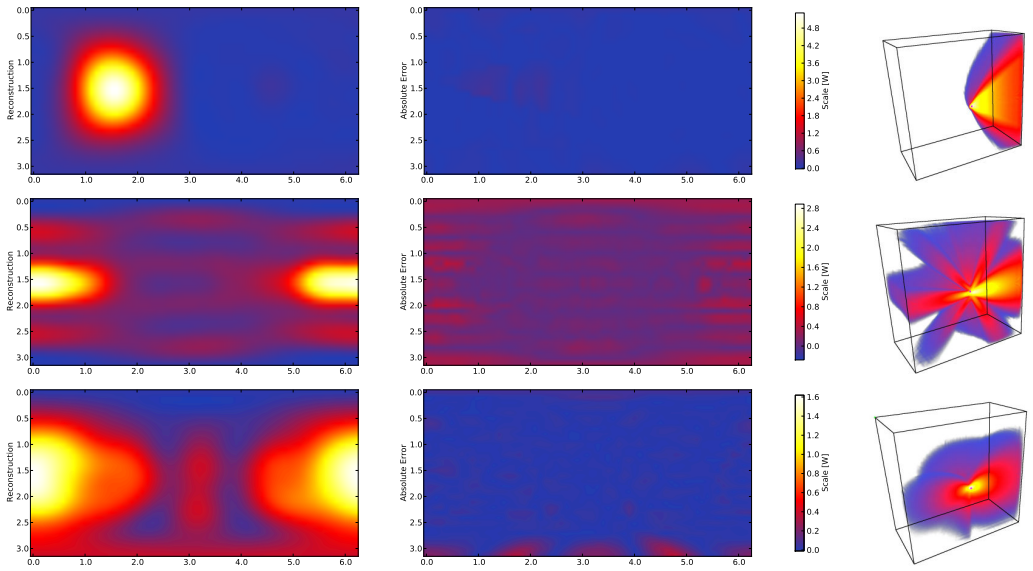

Fig. 1. Intensity plots of the three antenna patterns we used in our experiments. From top to bottom: Plaster, PULA, SPUCA. The plots show (from left to right) the reconstruction from the spherical harmonics, the absolute error between the measurement and the reconstruction and a volume rendering.

The coefficients can be used to reconstruct a low frequency approximation of the original function $f(s)$:

$$\tilde{f}(s) = \sum_{l=0}^{n-1} \sum_{m=-l}^{l} c_l^m y_l^m(s) \tag{3}$$

By constraining the degree of the reconstruction, we can achieve a compression of the original function. A low degree allows us to represent low frequency functions, such as relatively smooth antenna patterns. We use the SH representation for both the Tx and the Rx antenna, as well as for encoding the irradiance field at each voxel in our simulated environment.

IV. Antenna Patterns

The radiation pattern of an antenna significantly influences the link between two wireless stations. Simple dipole antennas radiate radially symmetric, with the highest gain orthogonally to the antenna. Other antenna designs allow a higher directionality and thus a higher efficiency and less interference with neighboring stations. Including such patterns in a propagation simulation adds to its accuracy.

Here we will describe how to efficiently incorporate arbitrary antenna patterns into a general ray tracing framework, and in particular into our photon path map algorithm [8].

The input for our work is some antenna pattern $a(\theta, \phi)$, measured using some probe that allows for measurement of the pattern in both azimuth ϕ and inclination θ. Typically about 8,000 samples are used for this. To get a continuous, compact and efficient representation we choose to use the spherical harmonics basis for approximating the antenna patterns. We use Equation (2) to compute a vector of coefficients for both the Tx and Rx antenna, using stratified Monte Carlo integration. Since the measured samples usually lie on a regular grid on the sphere and the Monte Carlo samples do not, we use the following algorithm for the projection. We do not use the measured samples, since we would have to estimate their distribution. Furthermore the Monte Carlo approach allows us to use arbitrary sample distributions.

We put all the measured samples in a kd-tree. Then we generate N stratified Monte Carlo samples $s_i \in \{0 \dots \pi\} \times \{0 \dots 2\pi\}$. For every sample, we compute an average $knn(s_i)$ of the k nearest neighbors. This gives us an interpolated function value of the measured pattern. We can then use Monte Carlo integration to compute the coefficient of level l and order m as:

$$c_l^m \approx \frac{4\pi}{N} \sum_{i=1}^{N} knn(s_i) y_l^m(s_i) \tag{4}$$

A. Transmitting Antenna

The main problem for all ray tracing based radio wave propagation algorithms is to generate rays on the Tx antenna, according to the antenna pattern. This amounts to a sampling problem of a probability distribution function (PDF) $p(\theta, \phi)$, which is proportional to the antenna pattern $a(\theta, \phi)$. The naïve approach would be to use rejection sampling. However this has two drawbacks. First, we need to know a bound on the maximum value that our antenna pattern will have. This can be computed from the measured samples and can be stored with the pattern. Second, rejection sampling is particularly inefficient and slow if the bounding function does not tightly enclose the function to be sampled. Usually one will use a sphere as the bounding function, and especially for highly directional antennas this will result in lots of samples to be rejected.

Instead we opt to implement the sample warping approach introduced by Jarosz et al. [9]. Here, we generate a uniform distribution of samples on the sphere. Then we recursively warp the samples according to the amount of energy contained in each quadrant of a 1:4 subdivision of the pattern in the

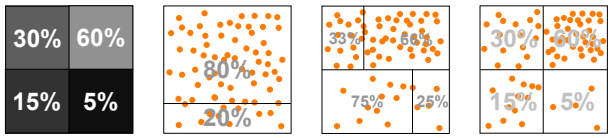

Fig. 2. Sample warping works by computing the relative magnitudes of the function values of a 1:4 subdivision and then doing one vertical, and one horizontal warping step.

(θ, ϕ) domain. We continue the recursion until a sufficient distribution quality is achieved, e.g. at most one sample per quadrant remains. One warping step is shown in Figure 2. Jarosz describes how to compute the energy contained in each quadrant by computing the integrals over the spherical harmonic basis functions. The warped samples are then used for generating the rays or photons. For an urban scenario we typically use around five million initial photons. Details of the photon path map algorithm can be found in our previous publications [10], [8].

B. Receiving Antenna

Assuming that the antenna pattern was measured with the antenna being fed a unit amount of energy, the pattern will represent the actual antenna gain in our model. Because of the reciprocity of the propagation path, we can take the same pattern both for the transmitting as well for the receiving role. When modeling the receiving antenna in the simulation, we can compute the gain $g(\theta, \phi)$ in a particular direction by using Equation (3):

$$g(\theta, \phi) = \sum_{l=0}^{n-1} \sum_{m=-l}^{l} c_l^m y_l^m(\theta, \phi) \tag{5}$$

In a typical ray tracing algorithm, where we construct one path from the transmitter to the receiver, we can use this to weight the incoming path with the antenna gain. In our photon path map algorithm, however we can use a different approach, which is explained in Section V.

C. Rotating the Antenna Pattern

Both the transmitting and receiving antenna need to be positioned and rotated in the simulation. For the Tx antenna, we could simply transform the generated rays by the rotation matrix. For the Rx antenna however we would like to rapidly move and rotate it, to interactively explore the simulation environment. Hence we need to rotate the whole antenna pattern in the spherical harmonic basis. We implemented the method described by Blanco [11], which is accurate and fast enough for our purposes. We use this method for both the Tx and the Rx antenna pattern. Also see the next section for how the transformed Rx pattern is used in the photon path map algorithm to evaluate the final signal strength.

A more simple approach can be used in a traditional ray tracer. When a path from the Tx to the Rx antenna has been created, the last path segment is simply transformed by the inverse rotation matrix, to put the ray path in the local coordinate system of the antenna. This is done using a standard 3×3 matrix once for each ray, instead of a set of $l \times l$ ($l \in 1 \ldots n$) matrices needed for a spherical harmonic rotation once for the simulation. Hence the SH rotation is more difficult to implement, but much more efficient in the end.

V. Encoding Irradiance

As previously said, a traditional ray tracer would compute propagation paths between a fixed Tx and Rx station. Our photon path map however computes the propagation of all rays emanating from a transmitting antenna. The result of the algorithm is a 3D buffer of voxels, each containing an average signal strength, or irradiance.

We now propose to extend this method to also include directionality. The goal is to encode the direction from which the propagation paths are coming. Again, we will use the spherical harmonics basis to store the incoming directions per voxel. The advantage is that it compresses the amount of data considerably. The disadvantage is however that it assumes rather smooth, slowly changing irradiance. Hence for each voxel we store spherical harmonics coefficients:

$$c_l^m = \frac{4\pi}{|V|} \sum_{p \in V} \Phi(p) \cdot y_l^m(\theta(p), \phi(p)) \tag{6}$$

Where V is the set of photons in the current voxel, p is a photon passing through the voxel and $\Phi(p)$ is the flux carried by this photon.

For every SH basis function we create a 3D buffer of coefficients. For evaluating the intensity of the received signal, we simply place the Rx antenna at the appropriate place in the 3D buffer and compute the total intensity s as received by the Rx antenna as:

$$s(x) = \int I_x(s) a_{\mathrm{Rx}}(s) ds = \langle c_x \,|\, c_{\mathrm{Rx}} \rangle \tag{7}$$

Where x is the point in space to be queried, I_x is the irradiance function, $a_{\mathrm{Rx}}(s)$ is the Rx antenna pattern, c_x is the vector of SH coefficients of the irradiance at this point, and c_{Rx} is the vector of SH coefficients for the Rx antenna. So the evaluation simply reduces to a scalar product of the two SH coefficient vectors.

VI. Results

We used three antenna patterns with very different characteristics for our experiments. The PULA and SPUCA patterns are by Schneider [12]. The plaster antenna pattern is by Kellomäki [13]. For each antenna we computed the spherical harmonic projection using 8,000 stratified Monte Carlo samples, using an average of the six nearest samples and using basis functions up to degree seven.

For comparison with Landmann et al. [1] we computed the normalized mean squared error (NMSE) as per their definition:

$$\mathrm{NMSE} = \frac{E((f - \tilde{f})^2)}{E(f)} \tag{8}$$

We also computed the unnormalized mean squared error (MSE). Both are displayed in Table I. Landmann et al. report

Pattern	MSE	NMSE
Plaster	-27.83 dB	-25.44 dB
PULA	-17.96 dB	-14.24 dB
SPUCA	-31.56 dB	-29.05 dB

TABLE I
MSE AND NMSE FOR THE THREE DATA SETS.

Pattern	Rejection Sampling	Warping
Plaster	43.29 sec	2.84 sec
PULA	21.45 sec	2.86 sec
SPUCA	12.69 sec	2.86 sec

TABLE II
THE PERFORMANCE OF THE RAY SAMPLING, FOR FIVE MILLION PHOTONS, SHOWING BOTH REJECTION SAMPLING AND THE SH WARPING METHOD.

a range of the NMSE of -15 to -30 dB for about 225 to 900 coefficients. For the same accuracy we only need 64 coefficients. Furthermore, our pattern accuracy is not depending on the antenna rotation, which is an advantage over the EADF method.

outdoor/

The plaster antenna pattern is very simple, consisting only of one main lobe. It can be approximated very well by the SH basis. The PULA pattern is much more difficult, since it contains several detailed components, which correspond to the higher frequency SH basis functions. This can be seen in Figure 1 in the absolute error plot. Here, the PULA pattern shows characteristic horizontal lines, which cannot be approximated by the SH basis functions of order seven. The SPUCA pattern on the other hand can be approximated very well.

One problem that appears with the spherical harmonic basis is the Gibbs phenomenon, or ringing. At certain, discontinuous points, the reconstructed function will show ripples. The same problem occurs with Fourier transformations and other basis functions and is not specific to our basis choice. This can lead to negative values in the reconstructed antenna pattern, and also influences the approximation quality in positive regions of the function. The negative values need to be filtered out, when using the pattern as a basis for a distribution function. This happens visibly in the PULA antenna pattern, but not in the other two patterns, since they are very smooth and can be approximated very well by the SH basis.

In Table II we show the performance of the ray sampling for the Tx antenna. The naive rejection sampling is 4-15 times slower than the SH warping method. Both methods were implemented on the CPU, taking advantage of all available cores (i7 920, QuadCore, 2.7GHz). The SH warping implementation of Jarosz on the GPU is even faster still. However the sampling performance is not the bottleneck in our algorithm, using the warping method. Tracing the rays and estimating the ray density now takes up almost all the computation time. The plaster antenna is a worst case for the rejection sampling, since it is highly directional, and thus many samples are rejected. The SH warping shows constant performance, independent of the pattern shape, which is expected.

In Figure 1 we show a volume rendering of all three data sets used. Again, we used our photon path map algorithm using five million photons. The rendering itself shows a cut through the 3D volume, rendered using our proprietary ray casting volume renderer, which allows us to explore the 3D volumes created by our simulations.

VII. CONCLUSION

We have presented a method to approximate antenna patterns in the spherical harmonics basis, and to incorporate them in a ray tracing propagation framework. Both the Tx and the Rx antenna can be modeled by our approach. The SH representation is very compact but still very accurate, as shown with our test data sets. Also we showed how to encode directional irradiance using the spherical harmonics basis. In the future, we would like to test our irradiance encoding against measured values, to see if the accuracy is good enough. However, measurements with directional resolution is difficult, so this remains an interesting problem.

ACKNOWLEDGMENT

This project was funded by the DFG Cluster of Excellence on Ultra-high Speed Mobile Information and Communication (UMIC), German Research Foundation grant DFG EXC 89. http://www.umic.rwth-aachen.de/

REFERENCES

[1] M. Landmann and G. Del Galdo, "Efficient antenna description for mimo channel modelling and estimation," in *Wireless Technology, 2004. 7th European Conference on*, 2004, pp. 217 – 220.

[2] J. Rahola, F. Belloni, and A. Richter, "Modelling of radiation patterns using scalar spherical harmonics with vector coefficients," in *European Conference on Antennas and Propagation*, 2009.

[3] H.-P. Chang, T. Sarkar, and O. Pereira-Filho, "Antenna pattern synthesis utilizing spherical bessel functions," *Antennas and Propagation, IEEE Transactions on*, vol. 48, no. 6, pp. 853 –859, Jun. 2000.

[4] A. Sheth, S. Seshan, and D. Wetherall, "Geo-fencing: Confining wi-fi coverage to physical boundaries," in *Pervasive*, ser. Lecture Notes in Computer Science, H. Tokuda, M. Beigl, A. Friday, A. J. B. Brush, and Y. Tobe, Eds., vol. 5538. Springer, 2009, pp. 274–290.

[5] J. Boerman and J. Bernhard, "Performance study of pattern reconfigurable antennas in mimo communication systems," *Antennas and Propagation, IEEE Transactions on*, vol. 56, no. 1, pp. 231 –236, 2008.

[6] F. Gunnarsson, M. Johansson, A. Furuskar, M. Lundevall, A. Simonsson, C. Tidestav, and M. Blomgren, "Downtilted base station antennas - a simulation model proposal and impact on HSPA and LTE performance," in *Vehicular Technology Conference, 2008. VTC 2008-Fall. IEEE 68th*, 2008, pp. 1 –5.

[7] R. Green, "Spherical harmonic lighting: The gritty details," in *Game Developers Conference*, 2003.

[8] A. Schmitz and L. Kobbelt, "Wave propagation using the photon path map," in *PE-WASUN '06*. New York, NY, USA: ACM, 2006, pp. 158–161.

[9] W. Jarosz, N. A. Carr, and H. W. Jensen, "Importance sampling spherical harmonics," *Comput. Graph. Forum*, vol. 28, no. 2, pp. 577–586, 2009.

[10] A. Schmitz and L. Kobbelt, "Efficient and accurate urban outdoor radio wave propagation," in *IEEE ICEAA*, September 2011.

[11] M. A. Blanco, M. Flrez, and M. Bermejo, "Evaluation of the rotation matrices in the basis of real spherical harmonics," *Journal of Molecular Structure: THEOCHEM*, vol. 419, no. 1-3, pp. 19 – 27, 1997. [Online]. Available: http://www.sciencedirect.com/science/article/pii/S0166128097001851

[12] C. Schneider, "Multi-user mimo channel reference data for channel modelling and system evaluation from measurements," in *Int. ITG Workshop on Smart Antennas*. EURASIP, February 2009.

[13] T. Kellomäki and W. Whittow, "Bendable plaster antenna for 2.45 GHz applications," in *Antennas Propagation Conference, 2009. LAPC 2009. Loughborough*, nov. 2009, pp. 453 –456.